Effective light absorption and absolute electron transport rates in the coral *Pocillopora damicornis*

Milán Szabó[a,#,*], Daniel Wangpraseurt[a,#], Bojan Tamburic[a], Anthony W.D. Larkum[a], Ulrich Schreiber[b] David J. Suggett[a], Michael Kühl[a,c], Peter J. Ralph[a]

[a]Plant Functional Biology and Climate Change Cluster, University of Technology, Sydney, Broadway 2007, NSW, Australia

[b]Julius-von-Sachs Institut für Biowissenschaften, Lehrstuhl Botanik I, Universität Würzburg, Germany

[c]Marine Biological Section, Department of Biology, University of Copenhagen, DK-3000 Helsingør, Denmark.

[#]These authors contributed equally to the present work

*Corresponding Author: Dr. Milán Szabó**,** Plant Functional Biology and Climate Change Cluster, Faculty of Science, University of Technology, Sydney, 745 Harris St. and 95 Thomas St. Ultimo 2007, NSW, Australia; PO Box 123, Tel.: +61-2-9514-4162, Fax: +61-2-9514-4079, Email: milan.szabo@uts.edu.au

Abbreviations

AL, Actinic light; E_d, Incident downwelling photon irradiance (400-700 nm); E_0(meas), Photon scalar irradiance within coral tissue (measured with microsensors, 400-700 nm); E_0(calc), Photon scalar irradiance within coral tissue (calculated based on $\sigma_{II}(\lambda)$); ETR, Electron transport rate of PS II (µmol electrons m^{-2} s^{-1}); ETR_{II}, Absolute rate of PSII turnover (electrons $PSII^{-1}$ s^{-1}); ETR_{II}^{max}, Maximum rate of PSII turnover (electrons $PSII^{-1}$ s^{-1}); FRRf, Fast Repetition Rate fluorometry; LC, Light curve of fluorescence parameters, defined as photosynthesis versus irradiance; MC-PAM, Multi-colour Pulse Amplitude Modulated fluorometer, NPQ, Non-photochemical quenching; $\sigma_{II}(\lambda)$, Wavelength-dependent absorption cross-section of PSII (nm^2) as determined by the MC-PAM fitting routine

Abstract

Pulse Amplitude Modulation (PAM) fluorometry has been widely used to estimate the relative photosynthetic efficiency of corals. However, both the optical properties of intact corals as well as past technical constrains to PAM fluorometers have prevented calculations of the electron turnover rate of PSII. We used a new multi-colour PAM (MC-PAM) in parallel with light microsensors to determine for the first time the wavelength-specific effective absorption cross-section of PSII photochemistry, $\sigma_{II}(\lambda)$, and thus PAM-based absolute electron transport rates of the coral photosymbiont *Symbiodinium* both in culture and *in hospite* in the coral *Pocillopora damicornis*. In both cases, σ_{II} of *Symbiodinium* was highest in the blue spectral region and showed a progressive decrease towards red wavelengths. Absolute values for σ_{II} at 440 nm were up to 1.5-times higher in culture than *in hospite*. Scalar irradiance within the living coral tissue was reduced by 20% in the blue when compared to the incident downwelling irradiance. Absolute electron transport rates of *P. damicornis* at 440 nm revealed a maximum PSII turnover rate of ca. 250 electrons $PSII^{-1}$ s^{-1}, consistent with one PSII turnover for every 4 photons absorbed by PSII; this likely reflects the limiting steps in electron transfer between PSII and PSI. Our results show that optical properties of the coral host strongly affect light use efficiency of *Symbiodinium.* Therefore, relative electron transport rates do not reflect the productivity rates (or indeed how the photosynthesis-light response is parameterised). Here we provide a non-invasive approach to estimate absolute electron transport rates in corals.

Keywords: chlorophyll fluorescence, electron transport rate, coral, light absorption, spectral attenuation

1. Introduction

Coral primary productivity reflects a key indicator of "reef health" (Hoegh-Guldberg et al. 2007) but is time-consuming and labour intensive to measure based on conventional gas-exchange techniques (e.g. Warner et al. 2011) and is further complicated by the close coupling of symbiont photosynthesis and respiration with host respiration (Kühl et al. 1995). Pulse-amplitude modulated (PAM) chlorophyll fluorometry and the Saturation Pulse method (reviewed in Schreiber, 2004) are rapid tools for assessing the photosynthetic capacity of corals both *in situ* and in the laboratory (Hill et al. 2004; Ralph et al. 1999; Warner et al. 2011). Typically, PAM measurements of coral photosynthesis rely on determination of the effective PSII photochemical efficiency, $\Delta F'/F_M'$, under known irradiance levels of actinic light (AL), which is often quantified as the incident photon irradiance of photosynthetic active radiation (PAR=400-700 nm). A relative measure of photosynthetic activity is then calculated in terms of the relative electron transport rates (rETR), $rETR = \Delta F/F_M \cdot PAR \cdot 0.42$, where $\Delta F/F_M$ stands for maximal quantum yield and 0.42 is the so-called "ETR factor", which is a constant value assuming that 84% of all light is absorbed (as for plant leaves) and that only half of all light absorbed is delivered to PSII for photochemistry (Schreiber et al. 2012). However, the actual amount of light absorbed for PSII photochemistry is unknown for the symbiont algae (*Symbiodinium* sp.) residing in corals, and also appears variable amongst different genetic types of *Symbiodinium* sp. and their growth condition (Hennige et al. 2009; Suggett et al. 2011), placing fundamental limitations on applying PAM measurements to yield absolute coral photosynthesis rates.

Light harvesting by PSII is governed by the absorption cross-section of PSII photochemistry (σ_{PSII}) and concentration of functional PSII units (Oxborough et al. 2012; Schreiber et al. 2012). Importantly, σ_{PSII} describes an absolute measure of the photon capture efficiency of PSII, which is directly related to the photochemical efficiency of PSII (Ley and Mauzerall, 1982) and thus is indicative of the biochemical nature and biophysical arrangement of pigments within the light harvesting antennae (e.g. Suggett et al. 2004). In the past σ_{PSII} has been determined routinely using fast repetition rate fluorometry (FRRf) or fluorescence induction and relaxation (FIRe) fluorometry (Kolber et al. 1998) that employ single turnover flashes to progressively reduce the primary quinone

electron acceptor, Q_A, whereby the rise kinetics from the minimum to maximum fluorescence yield, i.e., from fully oxidised to fully reduced state of Q_A, describes the effective absorption and hence σ_{PSII}.

To date, measurements of σ_{PSII} were mostly done with 'optically thin' microalgal samples (Koblizek et al. 2001; Schreiber et al. 2012; Schreiber and Klughammer, 2013; Suggett et al. 2004, 2009), including *Symbiodinium* cultures (Hennige et al. 2009, Ragni et al. 2010). The few published measurements of coral σ_{PSII} values show that σ_{PSII} for *Symbiodinium* sp. *in hospite* appears highly dynamic amongst coral species (Gorbunov et al. 2001; Hennige et al. 2011; Levy et al. 2003;), across water depth (Lesser 2000) and daytime (Gorbunov et al. 2001). Based on such PSII cross-sectional area determinations, the rate of photosynthetic electron transport per PSII reaction center was estimated in corals (Gorbunov et al. 2001).

The apparent 'plasticity' of σ_{PSII} in corals could play a key role in moderating absolute electron transfer rates and hence productivity in corals. It likely reflects differences in *Symbiodinium* genotype dominance since pigment properties (Hennige et al. 2009) and energetic connectivity amongst PSII reaction centres (Ragni et al. 2010, Hennige et al. 2011) is known to vary amongst sub-clades. Whilst these past measurements have demonstrated the inherent variability of σ_{PSII} in corals, they only involved measurements at a single wavelength and were not directly applicable to absolute production estimates without additional knowledge of the spectral dependency of PSII light harvesting. Light absorption by *Symbiodinium* is highest in the blue region (440-480 nm) due to the cumulative absorption of the photosynthetic pigments of chlorophyll *a*, c_2 and carotenoids. Past FRR and FIRe fluorometers were therefore designed to target peak absorption, and hence σ_{PSII}, in the blue (450-480 nm). Recent developments in chlorophyll fluorescence instrumentation, the Multi-colour Pulse Amplitude Modulated chlorophyll fluorometer (further referred as MC-PAM, Schreiber et al. 2012) however allows the determination of σ_{PSII} at multiple wavelengths across the visible spectral range, i.e also in the green (~560 nm) that is of special importance in dinoflagellates due to the light absorption by peridinin, located in their light-harvesting pigment-protein antenna complexes (see e.g. Iglesias-Prieto et al. 1993). The measuring principle for determining effective absorption of PSII with the MC-PAM is somewhat different from the approaches used in FRR and FIRe fluorometry (see above) and relies on so-called "O-I_1 induction kinetics" (Schreiber et al. 2012). Briefly, O-I_1 kinetics describe the photochemical phase in the polyphasic rise of PSII fluorescence at the onset of strong actinic illumination used to yield a O-I_1-I_2-P induction curve (Schreiber et al. 2004); another

nomenclature describes this as the O-J-I-P induction curve (Strasser and Govindjee, 1992). Both I_1 and J fluorescence yields mark the end of the photochemical and the start of the thermal induction phase but their determination and interpretation are somewhat different (Schreiber et al. 2012). I_1 is determined via a saturating single turnover flash applied at the end of the photochemical phase, which is driven by continuous actinic light (AL or MT). Following the saturating single turnover flash, Q_A is first fully reduced and then partially reoxidized with a time constant in the order of 300-400 µs. The I_1 level is determined by extrapolation to the end of the flash. While J is also determined at the end of the photochemical phase, it simply represents a single inflection or step in the induction curve, where light driven Q_A reduction and reoxidation via electron transfer to the secondary acceptor Q_B overlap; therefore, fluorescence yield corresponding to full reduction of Q_A^- cannot be precisely determined without application of a flash (Schreiber et al. 2012). Accurate analysis of the O-I_1 kinetics requires that changes in the original variable fluorescence yield are transformed into changes in Q_A reduction (PSII closure) by the equation $(F - F_0)/(I_1 - F_0) = (1 - q)/(1 + J\,q)$, with (1 - q) representing the fraction of closed PSII reaction centres and *J* being a measure of connectivity between PSII units (Lavergne and Trissl 1995).

The alternative measuring and analysis routines used in the MC-PAM as compared to FRR (FIRe) fluorometry requires specification of alternate terminology for the wavelength-dependent absorption cross-section of PSII, which was defined here as $\sigma_{II}(\lambda)$ (Schreiber and Klughammer, 2013). Using FRR/FIRe fluorometry, the $\sigma_{PSII}(\lambda)$ can be determined for any physiological state, notably different states of PSII reaction centre openness, redox conditions in the intersystem electron transport chain, membrane energisation, and state 1/state 2 conditions of the photosynthetic apparatus (e.g. Oxborough et al. 2012). It should be noted, however, that if $\sigma_{PSII}(\lambda)$ information is combined with information on the effective PS II quantum yield to estimate electron transport rate, care must be taken that e.g. NPQ by membrane energisation is not effective twofold by lowering PS II cross section as well as PS II quantum yield. In contrast, $\sigma_{II}(\lambda)$ as defined for measurements with the MC-PAM is only defined for a particular reference state, where Q_A and the plastoquinone (PQ) pool are oxidized, and non-photochemical quenching (caused by membrane energisation or state 2 formation) is absent (Schreiber et al. 2012). Thus, for calculation of electron transport rates, any loss in activity due to closure of PSII reaction centres or a decline in the efficiency of charge separation of

open reaction centres by non-photochemical quenching mechanisms is not accounted for via $\sigma_{II}(\lambda)$ but via the measured effective PSII photochemical efficiency, $\Delta F/F_M$ (Schreiber et al. 2011, 2012; see also Suggett et al. 2011). In our study, $\sigma_{II}(\lambda)$ refers to the intrinsic, maximal potential absorption cross-section of PSII at a given wavelength, measured under the same conditions under which the PSII photochemical efficiency is at its maximum (i.e., $\Delta F/F_M$). In its original definition, this intrinsic $\sigma_{II}(\lambda)$ can be determined in optically thin samples only, i.e., in the absence of wavelength-dependent light gradients. However, the present study explores its possible application in opaque samples such as thin-tissued corals. In surface-associated phototrophs such as corals, the optical properties of the host system strongly modulate the actual light availability of zooxanthellae *in hospite* (Enriquez et al. 2005; Kühl et al. 1995; Teran et al. 2010; Wangpraseurt et al. 2012, 2014). Coral tissue and the coral skeleton are both strong scatterers (Marcelino et al. 2013; Wangpraseurt et al. 2014), and as scattering increases the path length of photons per vertical distance travelled it can lead to a local enhancement in scalar irradiance over the incident downwelling irradiance (Wangpraseurt et al. 2012). Steep light gradients exist within the coral tissue, where scalar irradiance can attenuate by one order of magnitude or more from the tissue surface to the skeleton. Light attenuation of photosynthetically active radiation (PAR) within the tissue is wavelength dependent due to the presence of host pigments and symbiont photopigments, where the blue spectral region is attenuated to a larger extent than red light (Wangpraseurt et al. 2012). Substantial distortions of photosynthesis vs. irradiance curves and photosynthetic action spectra can thus be observed when relating coral photosynthesis to incident irradiance instead of the actual scalar irradiance (Kühl et al. 1995).

In this study, we determine the first spectrally-resolved measurements of $\sigma_{II}(\lambda)$ in an important reef building coral species, *Pocillopora damicornis*. We subsequently evaluate these properties alongside measurements of the light microenvironment within the coral tissues to assess the role of tissue optics in affecting light availability and hence $\sigma_{II}(\lambda)$. These data are finally applied to yield absolute electron transport rates based on calculations of the effective light field in coral tissue.

2. Methods

2.1. Experimental material

168 Specimens of the branching coral *Pocillopora damicornis* were collected from the reef flat (1-2m
169 depth) of Heron Island, in the southern Great Barrier Reef of Australia (151˚55'E, 23˚27'S) and were
170 transported to the coral holding facility of the University of Technology Sydney. Here, all colonies
171 were maintained in tanks provided with artificial seawater (prepared with 'Ocean Nature' sea salt,
172 Aquasonic) that was circulated through a natural biological sump. Tanks were provided with an
173 incident photon irradiance of 50-70 µmol photons m^{-2} s^{-1} (250W metal-halide lamps, Aqualine, Aqua
174 Medic Inc., colour temperature 13,000K) set to a 14h:10h day:night cycle at a constant temperature of
175 26˚C. Corals were fragmented into nubbins with a surface area of ~1 cm^2 two days prior to the
176 experiment and kept in the same aquaria under essentially the same light conditions.
177 *Symbiodinium* sp. (Australian National Algae Culture Collection, ANACC, strain CS-73, originally
178 isolated from Heron Island, in the southern Great Barrier Reef of Australia) was cultured in f/2 medium
179 (Guillard et al. 1975) in Erlenmeyer flasks under a downwelling photon irradiance of 30-40 µmol
180 photons m^{-2} s^{-1} (TLD 18W/54 fluorescent tubes, Philips, colour temperature 10,000K) using the same
181 irradiance cycle and water temperature as per the coral specimens. Cultures were maintained in
182 exponential growth phase for 14-18 days prior to harvesting. Comparative measurements of $\sigma_{II}(\lambda)$
183 were performed on freshly isolated *Symbiodinium* cells from the tissues of *P. damicornis* (Hill et al.
184 2009). However, as the freshly isolated symbionts exhibited suboptimal $\Delta F/F_M$ values that were ~20%
185 lower than in cultured or in hospite *Symbiodinium* (data not shown), we propose that these
186 preparations cannot be precisely used as a reference $\sigma_{II}(\lambda)$ for *Symbiodinium* sp. in our calculations.

187

188 2.2. Experimental setup

189 Variable chlorophyll fluorescence measurements were performed with a MC-PAM (Heinz-Walz
190 GmbH, Effeltrich, Germany) equipped with either (i) an optical unit designed for leaf measurements
191 (MCP-BK, Heinz-Walz GmbH) for measurements on intact coral nubbins, or (ii) an optical unit with a
192 central quartz cuvette (ED-101US/MD) for measurements on cell suspensions of *Symbiodinium* sp. In
193 the case of the MCP-BK optical unit the optical guide rod (Perspex) for fluorescence excitation points
194 to the specimen almost perpendicularly (12° angle of incidence) and tapers from 10 x 10 mm at the
195 emitter site to 6 x 6 mm at the measuring point. The optical guide rod (Perspex) for fluorescence
196 detection has constant edge lengths of 10 mm and collects fluorescence at a rather large angle of

incidence. The optical unit ED-101US/MD consists of a centrally located place for a 10 x 10 mm cuvette and perpendicularly positioned ports for the optical guide rods for the emitter and detector heads of the MC-PAM. Coral nubbins were housed in the measuring chamber (a glass cuvette with dimensions of 45 x 40 x 10 mm), which was placed adjacent to the LED light source in the leaf clip setup. The position of coral nubbins within the chamber was carefully adjusted with a micromanipulator (MM33, Märzhäuser GmbH, Wetzlar, Germany) in order to place a nubbin directly in the light path of the fluorometer. Throughout the measurements, coral nubbins were kept in the measuring chamber filled with seawater under continuous aeration provided by a glass Pasteur pipette attached to an air pump (Precision 9500, Aqua One, Ingleburn NSW, Australia). The aeration was adjusted to ~3 bubbles/s with a bleed valve that was inserted in the aeration line from the air pump to the measuring cuvette. The temperature was kept constant at 26˚C using a temperature control unit (US-T, Heinz-Walz GmbH, Effeltrich, Germany). *Symbiodinium* cultures were kept in the quartz cuvette of the ED-101US/MD unit under continuous stirring using a small magnetic stir bar (Heinz-Walz GmbH, Effeltrich, Germany).

2.3. Establishment of PAR lists

A full set of PAR lists contains data of photosynthetically active radiation (PAR; µmol photons m^{-2} s^{-1}), for all wavelengths and intensity settings of actinic illuminations (AL) and multiple turnover flashes (MT). As the three-dimensional curved geometry of the coral nubbins cannot be compared to the flat surface of a leaf, the PAR lists normally established by using a downwelling quantum irradiance sensor for leaves (US-MQS, Walz GmbH) were not applicable in our study. Moreover, we found considerable light inhomogeneity along the measuring head (see below), which would likely result in an incorrect estimation of incident PAR. Therefore, a quantum scalar irradiance sensor (US-SQS, Walz GmbH) was used to cross-calibrate the US-MQS sensor used to establish PAR list for the optical unit MCP-BK as follows. Both sensors were placed in the same orientation as for the sample holder used to calibrate PAR list during leaf measurements. The US-MQS sensor was placed in the leaf clip and into the middle of the emitter-detector Perspex rod pair, which serves as a light guide from the “Chip-On-Board” excitation source in the emitter unit to the photodiode in the detector unit. The light-collecting tip of the US-SQS sensor was carefully placed in the same location using a micromanipulator (MM33, Märzhäuser GmbH, Wetzlar, Germany). Using 440 nm actinic light (AL) at

setting 20, and with both sensors kept at 1 mm distance from the centre of the emitter-detector light guide pair, a photon irradiance of 2730 µmol photons m^{-2} s^{-1} was measured by both sensors. Placing the US-SQS sensor in the same measurement configuration in the optical glass cuvette filled with seawater, the sensor was further carefully adjusted with the micromanipulator to different positions relative to the emitter light guide rod: the centre, the four corners, the edge, and the middle of the emitter and detector light guide rods. The calibration factor of the US-SQS sensor was adjusted for the water immersion effect. The PAR list was then recorded at each position. Significant heterogeneities in the light field could be quantified across a 10x10 mm square, i.e., representing the area of coral nubbins that were later placed in front of the MC-PAM optical unit. The highest variance was observed when PAR lists at the edges of emitter and detector light guide rods were compared (differing by a factor of two). Therefore, to maximise the accuracy of incident PAR calibrations, a 3.5x5 mm aperture was mounted in front of the optical unit and adjusted so that the PAR obtained via the calibration process remained homogeneous at ~1580 µmol photons m^{-2} s^{-1} using 440 nm AL at setting 20. The PAR list established in this way was used for all coral measurements in this study. PAR lists in the cuvette system were subsequently verified using a spherical micro-quantum sensor (US-SQS/WB, Heinz-Walz GmbH, Effeltrich, Germany) according to (Schreiber et al. 2012).

2.4. Measurement protocol

Coral nubbins and cell suspensions were dark-acclimated for 15 min in the presence of weak far-red light (setting 2 on the MC-PAM) to ensure oxidation of the intersystem photosynthetic electron transport pool and obtain a defined reference state for chlorophyll fluorescence measurements of the PSII maximum photochemical efficiency ($\Delta F/F_M$) and the PSII absorption cross-section ($\sigma_{II}(\lambda)$). $\Delta F/F_M$ was quantified via application of a strong saturating light pulse (intensity: 3500-4000 µmol photons m^{-2} s^{-1}, width: 0.6s), followed by a dark acclimation period of 1 min. A pre-programmed script optimised for coral nubbins (see below 'Determination of functional absorption cross-section of PSII') was then applied according to Schreiber and Klughammer (2013) to determine $\sigma_{II}(\lambda)$ sequentially for five wavelengths: 440, 480, 540, 590 and 625 nm. A further 5 min of dark-acclimation in the presence of weak far-red was applied to ensure full oxidation of the PQ-pool followed by an automated steady-state light curve (SSLC) with 3 min incubation at each irradiance to examine the light response of the

PSII photochemical efficiency ($\Delta F'/F_M'$) of the effective PSII quantum yield. The SSLC comprised of a series of increasing irradiance of a specific wavelength (here the 440 nm LED), with data recorded via Light Curve Program files (lcp-files, Schreiber et al. 2012). The lowest irradiance levels (<10 µmol photons m^{-2} s^{-1}) were generated by using the MC-PAM measuring light (ML) at high pulse frequency settings (1000-2000), where the same colour ML was used as per the AL. Three replicates were run using a new nubbin for each measurement. Data are thus shown as averages ± standard error (S.E.) of three independent biological replicates of *P. damicornis* nubbins.

2.5. Measurements of wavelength-dependent absorption cross-section of PSII

A pre-programmed fast kinetic trigger file of the MC-PAM system (Sigma500.FTM) was used for automated measurements of fast fluorescence induction kinetics according to Schreiber and Klughammer (2013). Consecutive O-I_1 rise kinetics were recorded for each LED colour (440, 480, 540, 590 and 625 nm) using pre-programmed script files, which define wavelength-specific intensities of ML and AL (or multiple turnover light pulses), as well as the amplifier gain and the time intervals between the start of various trigger files (these scripts are available from the primary author upon request).

The optimisation process for obtaining reliable $\sigma_{II}(\lambda)$ values for nubbins of *P. damicornis* consisted of two steps. Firstly, the ML intensity and gain were adjusted to obtain similar minimal fluorescence (F_0) values, which facilitate a comparison of the rise kinetics. Secondly, the intensity of actinic light or multiple turnover light pulses were adjusted to obtain similar initial rise kinetics of the O-I_1 curves for all colours. When initial slopes are identical, differences in PAR are directly proportional to changes in $\sigma_{II}(\lambda)$. The $\sigma_{II}(\lambda)$ values were derived using a dedicated fitting routine provided by the PamWin-3 software (Heinz-Walz GmbH, Effeltrich, Germany) according to Schreiber et al. (2012). The fitting is based on the reversible radical pair model of PSII originally described by Lavergne and Trissl (1995) extended to take into account Q_A^- reoxidation (Schreiber et al. 2012). The free-fitting parameters in this model that are fitted by the PamWin-3 program, are i) J, a connectivity parameter (Lavergne and Trissl 1995), ii) τ, the time constant of light-driven reduction of Q_A (by actinic light or multiple turnover pulses), and iii) τ(reox), the time constant of Q_A^- reoxidation. Additional parameters F_0 and I_1 (O and I_1 levels in the PAM fluorescence induction terminology) are directly measured to define the variable

fluorescence (ΔF) that can be induced by a combination of strong continuous light (AL) or multiple turnover pulse (MT) and a single turnover saturating flash (ST pulse). The measurement is routinely carried out in the presence of weak far-red light (peaking at 735 nm), i.e., when the PQ pool is oxidised. The O-I_1 curves recorded with the five colours were fitted simultaneously with fixed *J* and τ(reox) parameters. As *J* and τ(reox) are intrinsic dynamic properties of PSII, they should not be influenced by the colour of light used for induction. Fluorescence was recorded at 665 nm using a RG long-pass emission filter in front of the MCP-D detector head.

2.6. Direct measures of light field within coral tissue

To directly measure the scalar irradiance within coral tissue (E_0(meas)) we used scalar irradiance microsensors (Lassen et al. 1992) as described previously (Wangpraseurt et al. 2012). Briefly, coral fragments were placed in a black flow-through chamber supplied with seawater (25 ºC; flow velocity ~3 cm s^{-1}) and illuminated with a downwelling photon irradiance of 400 µmol photons m^{-2} s^{-1}. Scalar irradiance was recorded within coenosarc tissue, i.e., the connective tissue in between polyps measuring light microprofiles from the skeleton surface upwards into the tissue surface. Prior to each scalar irradiance measurement, a micro-incision was made with a micro-needle (effective tip size <50 µm; ProSciTech Pty Ltd, USA) to allow smooth sensor penetration through the tissue. Five replicate profiles were carried out on randomly chosen coenosarc tissues of *P. damicornis*. Spectral data was recorded with the scalar irradiance microsensors connected to a fibre-optic spectrometer (USB2000+, Ocean Optics, Dunedin, FL, USA) controlled by the manufacturer's software (*Spectrasuite*). Scalar irradiance measurements were normalised to the incident downwelling irradiance (E_d), as measured with the microsensor positioned in the collimated light beam above a black non-reflective surface.

2.7. Calculation of $\sigma_{II}(\lambda)$

$\sigma_{II}(\lambda)$ for the intact coral and the *Symbiodinium* culture were calculated according to Schreiber et al. (2012) as:

$$\sigma_{II}(\lambda) = \frac{1}{\tau \cdot N_A \cdot E_d} \quad (1)$$

where $\sigma_{II}(\lambda)$ (nm^2) is the intrinsic wavelength-dependent functional absorption cross section of PSII (in optically thin suspension) or the apparent wavelength-dependent functional absorption cross section of PSII (in intact corals). Here, τ is the time constant of light-driven Q_A^- reduction (ms) determined from the fast fluorescence kinetics measurements (see above), N_A = Avogadro's constant ($6.03 \cdot 10^{23}$ quanta [mol photons]$^{-1}$), and E_d (µmol photons m^{-2} s^{-1}) is the incident downwelling irradiance that was kept equal in the coral and culture experiments.

2.8. Theoretically derived scalar irradiance within coral tissue

We theoretically derived the effective scalar irradiance within the coral tissue by assuming that in first approximation any change in $\sigma_{II}(\lambda)$ between coral and culture is caused by differences in the coral tissue scalar irradiance with respect to incident irradiance at a given wavelength, i.e., $\Delta\sigma_{II} = \Delta E$. Therefore we calculated the ratio of σ_{II}(coral)/σ_{II}(suspension) at each wavelength (440, 480, 540, 590 and 625 nm) and subsequently used the average value (n= 5-6) of the σ_{II}(coral)/σ_{II}(suspension) ratio to calculate the effective PAR at a given wavelength (λ) as:

$$E_0(\text{calc}) = E_d \cdot \sigma_{II}(\text{coral})/\sigma_{II}(\text{suspension}) \quad (2)$$

This equation is valid only if it is assumed that all cells involved in fluorescence measurements are exposed to the same scalar irradiance intensity. This assumption is likely only justified for the topmost layers of tissue which is monitored via short-wavelength fluorescence. However, if excited within deeper layers, the fluorescence signal is likely to become re-absorbed. We propose that potential errors in $\sigma_{II}(\lambda)$ calculations are minimised when strongly-absorbed 440 nm light is used (Schreiber et al. 2011). Therefore, recordings of light response curves with determinations of photon absorption rate of PSII (PAR_{II}) and electron turnover rate of PSII (ETR_{II}) were carried out using 440 nm light (see below).

2.9. Photon absorption rate of PSII (PAR_{II}) and electron turnover rate of PSII (ETR_{II})

The wavelength-dependent quantum absorption rate of PSII (PAR_{II}, photons $PSII^{-1}$ s^{-1}), which is equivalent to the photosynthetically usable radiation, was calculated as

$$PAR_{II} = s_{II} \times N_A \times PAR \quad (3)$$

where PAR is either E_d, E_0(calc) or E_0(meas). The wavelength-dependent absolute electron turnover rate of PSII, ETR_{II} was thus calculated as

$$ETR_{II} = PAR_{II} \cdot \left[\frac{\Delta F' / F_M'}{\Delta F / F_M} \right] \quad (4)$$

where $\Delta F'/F_M'$ is the effective quantum yield of PSII (in the light-adapted state), and $\Delta F/F_M$ is the maximal quantum efficiency of PSII (determined in the dark-adapted state with weak far-red background light). The ETR parameters ETR_{II}^{max} and E_k(II) were determined using the curve fitting protocol of PamWin-3.

2.10. Absorption measurements

Optical absorption spectra for *Symbiodinium sp.* were recorded by using a custom built spectrophotometer composed of a Tungsten-Halogen light source (LS-1, Ocean Optics), and a fibre optic spectrophotometer (USB2000, Ocean Optics) interfaced with an integrating sphere (FOIS-1, Ocean Optics) (see details in Petrou et al. 2013). *Symbiodinium* cells were filtered to GF/F filter paper (Whatman) which was placed directly in the light path of the Tungsten-Halogen lamp and across the collection port of the integrating sphere Absorption spectra were recorded using Spectra Suite software (Ocean Optics). Reference spectra were taken on clean filter paper filtered only with f/2 medium. Spectra were averaged (n=4) to increase S/N ratio and the average spectrum is shown along with the standard error (S.E.) at 440, 480, 540, 590 and 625 nm (Fig. 1).

3. Results

3.1. Wavelength-dependent absorption cross-section of Photosystem II ($\sigma_{II}(\lambda)$) of *Symbiodinium* for intact corals and cultures

Wavelength-dependent variations of σ_{II} were similar for *Symbiodinium* harboured in *P. damicornis* and in culture, with highest values in the blue and a progressive decrease towards the red end of the spectrum (Fig.1). However, the absolute values of σ_{II} differed between intact corals and *Symbiodinium* culture with mean σ_{II} values of ~6.5 and ~4.5 at 440 nm for cultured *Symbiodinium* cells and *P. damicornis* nubbins, respectively (Fig. 1). For *P. damicornis*, $\sigma_{II}(\lambda)$ values were ca. 20-30% lower between 440-540 nm (paired t-test, $p<0.05$), but ca. 15% higher at 590 nm than for cultured *Symbiodinium*. However, it should be noted that these differences at 590 nm were not statistically significant ($p<0.05$). In contrast, mean σ_{II} values in coral and culture were identical at 625 nm ($p>0.05$). The absorption spectrum of cultured *Symbiodinium* followed closely the shape of the $\sigma_{II}(\lambda)$ (Fig. 1), although the relative values differed when both spectra were normalised to their maximal levels. The corresponding data of the O-I_1 kinetic rise that were used for σ_{II} calculations are shown in Table 1, which shows that largely different PAR values were adjusted at different wavelengths to attain nearly identical τ values.

3.2. Effect of light microenvironment on $\sigma_{II}(\lambda)$ of *Symbiodinium*

Microscale spectral scalar irradiance at and within the tissue surface revealed strong spectral distortion from the incident downwelling irradiance (E_d), indicating that *Symbiodinium* in the intact coral and in suspension are subject to different light regimes (Fig. 2). Most pronounced was the red-shifted enhancement in tissue scalar irradiance relative to E_d. To assess whether differences in σ_{II} between coral and suspension translated to differences between the light field of the dilute suspension (i.e. E_d) and the light field within the intact coral [E_0(meas)] we also examined the ratio of σ_{II}(coral)/σ_{II}(suspension) vs. E_0(meas)/E_d (Fig. 2). The relative differences in σ_{II}(coral)/σ_{II}(suspension) followed closely (5-10% deviation) the differences in light availability for *Symbiodinium* in the intact coral vs. culture in the blue-green and red spectral region (Fig. 2). However, in the orange-red region (590-625 nm), the differences between coral and culture did not match well with measured differences in σ_{II} (offset between PAR and σ_{II}) of ~20-40% (Fig. 2).

3.3. Absolute electron transport rates of *Symbiodinium* in intact corals

398 Absolute electron transport rates under 440 nm light were determined for intact corals using full
399 downwelling irradiance (E_d) or measured scalar irradiance within the tissue (E_0(calc)) for PAR in
400 equation 3 (Fig. 3). Based on $E_{d,}$ the mean ETR_{II}^{max} was 370 electrons $PSII^{-1}$ s^{-1} (± 30 S.E.) and the
401 mean E_k(II) was 402 (± 37 S.E.) photons $PSII^{-1}$ s^{-1}. As expected, when based on $E_{0,}$ both the mean
402 ETR_{II}^{max} and E_k(II) were substantially lower at 261 electrons $PSII^{-1}$ s^{-1} (± 35 S.E.) and 248 (± 33 S.E.)
403 photons $PSII^{-1}$ s^{-1}, respectively. The 1.4 factor of difference between E_d and E_0(calc) reflects the ratio
404 of intrinsic σ_{II} (measured with an optically thin suspension of *Symbiodinium*) and the apparent σ_{II}
405 determined with the intact coral (see Table 1).

406

407 3.4. Effect of scalar irradiance within the coral on relative electron transport rates of *Symbiodinium*

408 In most studies, rETR values are calculated with the unrealistic assumption that a constant fraction
409 of incident PAR is absorbed by the sample, independent of the colour of applied light and the actual
410 absorption of this light in the sample. Nevertheless, measurements of rETR have proven useful for
411 many practical applications to analyse relative changes in photosynthetic performance in particular
412 species of corals, as long as the wavelength of light available (and the fundamental absorption
413 properties) remained constant. When rETR curves of the intact coral *P. damicornis* based on E_d were
414 compared with rETR curves based on E_0(calc) the LCs showed different maximal relative electron
415 transport rates ($rETR_{max}$ of 36 ± 2 and 26 ± 2, respectively) and an onset of saturation at different
416 irradiance levels (E_k of 143 ± 16 and 91 ± 11 µmol photons m^{-2} s^{-1}, respectively; Fig. 4).

417

418 **4. Discussion**

419 Our data demonstrate the wavelength dependency of the absorption cross section of PSII for
420 *Symbiodinium* in culture and *in hospite*. This comparison is essential to determine the effective
421 *Symbiodinium* light absorption properties *in hospite* that can be used to estimate absolute electron
422 transport rates in intact corals. Our measurements of $\sigma_{II}(\lambda)$ confirm past accounts of the spectral
423 dependency of absorption that were based solely on fluorescence excitation spectra of PSII
424 absorption from various *Symbiodinium* genotypes (Hennige et al. 2009).

425 The wavelength-dependent character of $\sigma_{II}(\lambda)$ reflects the unique pigment composition of
426 *Symbiodinium* sp. The most pronounced difference was the high functional absorption in the green
427 spectral region relative to the blue spectral region, which is indicative of a strong absorption of
428 peridinin, the main light harvesting carotenoid of *Symbiodinium* (Fig. 1). These findings are supported
429 by the absorption spectrum of *Symbiodinium* cultures (Fig. 1) and are in good agreement with
430 previous results showing the absorption and fluorescence excitation spectrum of various clades, i.e.,
431 the energy absorbed in the blue (440-480 nm) region is partitioned to PSII-specific absorption to a
432 larger extent than in the orange-red region (590-625 nm) (Hennige et al. 2009).
433 This spectral dependency of $\sigma_{II}(\lambda)$ is important when considering how *Symbiodinium*
434 photosynthesis is driven by light quality. Several previous studies have shown that blue light affects
435 coral photosynthetic parameters differently than red light (e.g. Kinzie et al. 1984; Levy et al. 2003;
436 Mass et al. 2010). For example, Levy et al. (2003) used FRR fluorescence to show that blue light
437 decreases the effective quantum yield to a greater extent than red light. These results correspond to
438 the differences of σ_{II} in blue vs. red parts of the spectrum reported here (Fig. 1) and indicate that 440
439 nm light is ~3.4-fold more efficiently utilised than 625 nm light in *Symbiodinium*.
440 We found that $\sigma_{II}(\lambda)$ of *Symbiodinium* harboured in *P. damicornis* showed a similar wavelength-
441 dependency as the cultured *Symbiodinium*, but that the absolute $\sigma_{II}(\lambda)$ values differed significantly
442 between the two types of symbiont environment (Fig. 2). Such deviation of the *apparent* $\sigma_{II}(\lambda)$ of *P.*
443 *damicornis* from the *intrinsic* $\sigma_{II}(\lambda)$ of a dilute *Symbiodinium* sp. is a result of the lowering of the mean
444 effective PAR within the coral tissues which increases with extinction. Similarly, Schreiber and
445 Klughammer (2013) observed lower $\sigma_{II}(\lambda)$ values for intact plant leaves (Dandelion) compared to
446 green algal cultures (*Chlorella*) and suggested that reduced $\sigma_{II}(\lambda)$ values are due to part of the
447 incident light being absorbed within the leaf and that such attenuation is most pronounced at
448 wavelengths of strong absorption, i.e., blue and red in higher plants chloroplasts. In a more recent
449 study, a thorough characterisation of $\sigma_{II}(\lambda)$ in optically dilute and dense *Chlorella* suspensions showed
450 that for optically dense cell suspensions, *apparent* $\sigma_{II}(\lambda)$ has to be distinguished from *intrinsic* $\sigma_{II}(\lambda)$,
451 with the latter corresponding to the value best measured with an optically thin cell suspension
452 (Klughammer and Schreiber, submitted to Photosynthesis Research).
453 The experimental procedure for determinations of *apparent* $\sigma_{II}(\lambda)$ and *intrinsic* $\sigma_{II}(\lambda)$ is
454 identical; however, $\sigma_{II}(\lambda)$ values cannot be determined with the same precision as intrinsic $\sigma_{II}(\lambda)$ values

since the underlying O-I_1 kinetics are the sum of many different components, as induced by a gradient of light intensities experienced by all cells within the optically-dense sample that ultimately contribute to the fluorescence signal. As noted above, it may be assumed that the reduction of *apparent* $\sigma_{II}(\lambda)$ with respect to *intrinsic* $\sigma_{II}(\lambda)$ is a measure of the reduction of the mean effective PAR with respect to incident PAR for the cells where fluorescence is measured. Importantly the measured effective quantum yield is representative for the same population of cells. Thus the MC-PAM allows us to obtain estimates of paired values of wavelength-dependent effective PAR and $\Delta F'/F_M'$ under identical conditions, from which absolute electron transport rates can be calculated.

Our light microsensor measurements within the intact coral suggest that differences in apparent $\sigma_{II}(\lambda)$ between corals and *Symbiodinium* culture are mainly due to differences in the light microenvironment of *in hospite* zooxanthellae. In the blue part of the spectrum, relative differences in $\sigma_{II}(\lambda)$ between coral and culture correlated closely with respective differences in light availability (Fig. 3). However, towards the red part of the spectrum (590-625 nm), light availability itself was insufficient to explain the differences in $\sigma_{II}(\lambda)$ between coral and culture (Fig. 3). The reason for this mismatch remains unknown, but could be related to the configurational differences of microsensor and chlorophyll fluorescence measurements, as discussed in the following section.

Since fluorescence is measured by the MC-PAM predominantly from a defined subsurface layer of photosymbionts, which is thinner than the microsensor tip, there is an intrinsic difference between the theoretical scalar irradiance calculated from differences in $\sigma_{II}(\lambda)$ as compared to measured scalar irradiance values that will average over a larger tissue volume. In cases of very thin coral tissue, it cannot be ruled out that the small white light collecting sphere of the microsensor substitutes for a substantial part of tissue that normally contributes to light absorption, which would thus affect the tissue light field. However, in the case of very thin tissue, such potential measurement artefact may also be masked by increased diffuse reflectance of the tissue light field from the underlying coral skeleton. Other comparisons of calculated and measured scalar irradiance measurements indicate that such artefact is likely negligible in strongly scattering sediment (Kühl and Jørgensen 1994). Additional reasons explaining these discrepancies could be (i) the presence of host pigments that might have additional effects on coral photosynthesis e.g. due to spectral conversion (Dove et al. 2008, Smith et al. 2013), (ii) differences in the penetration depth of the PAM excitation light (i.e. measuring and actinic light), (iii) imbalance of excitation energy that arrives in PSII or PSI,

485 which was shown to be wavelength dependent in *Symbiodinium* (Hennige et al. 2009) or iv) other
486 factors that could lead to physiological differences of cultured and *in hospite Symbiodinium* such as
487 differences in the physico-chemical microenvironment of free-living and symbiotic *Symbiodinium* cells.

488 Despite these differences in microsensor and $\sigma_{II}(\lambda)$ data, both approaches revealed the same
489 magnitude of light attenuation in the blue and blue-green spectral region, which thus allowed for
490 estimating absolute electron transport rates in the blue region. Absolute electron transfer rates at 440
491 nm based on E_0(calc) and E_0(meas) were similar and both were approximately 40% lower than the
492 rates estimated when using E_d (Fig. 3). Interestingly, an ETR_{II}^{max} value of ca. 220-250 electrons $PSII^{-1}$
493 s^{-1} corresponded to PAR_{II} values (i.e. photon absorption rate) of ca. 1000 photons $PSII^{-1}$ s^{-1}, when
494 PAR_{II} was based on E_0(calc) or E_0(meas) (Fig. 3); PAR_{II} of 1000 photons $PSII^{-1}$ s^{-1} (= 1 photon $PSII^{-1}$
495 ms^{-1}) corresponds to a rate of Q_A^- reduction of ~1 ms^{-1} under reference conditions. Consequently, at
496 the maximum steady state ETR_{II}, PSII turns over approximately once for every 4 photons absorbed by
497 PSII (equivalent to 1 electron transported by PSII per 4 ms) reflecting the limiting step between PSII
498 and PSI at the protolytic reaction between PQH_2 and the Cyt b_6/f complex. Similar ETR_{II}^{max} rates have
499 been observed from the single-celled photosynthetic model organism *Chlorella* grown under a similar
500 light environment (Schreiber et al. 2012). The similarity of ETR_{II}^{max} values in the intact coral and
501 *Chlorella* in dilute suspension suggests that photosynthetic electron transport is limited by the same
502 partial reaction, i.e., most likely the protolytic step between PQH_2 and Cyt b_6/f (see above).

503 Together, these results have important implications for our understanding of coral photobiology.
504 Firstly, the optical properties of the coral host environment strongly affect the photon absorption rate
505 of *Symbiodinium* and secondly, the MC-PAM approach facilitates a reliable estimation of such rates in
506 a non-invasive and rapid manner. Our results also have implications for the determination of the light
507 saturation irradiance, E_k, commonly derived from rETR vs. irradiance measurements. For instance,
508 we found that if coral optical properties are not taken into account, E_k was overestimated by ca. 40%
509 (Fig. 4), thus further highlighting the value of coral tissue optics data for improving accuracy of not
510 only photosynthesis rates but also photosynthesis-irradiance parameterisation, i.e., estimates in line
511 with earlier findings comparing P vs. E curves and action spectra using downwelling versus scalar
512 irradiance as measures of the actinic light levels in coral tissue (Kühl et al. 1995).

513 In conclusion, we resolved the wavelength dependency of the functional absorption cross-
514 section of PSII in *Symbiodinium* and provided the first PAM-based measures of absolute electron

transfer rates in intact corals. The optical properties of coral tissues have a central role in affecting the photosynthetic performance of *in hospite Symbiodinium* and our study implies that knowledge of coral tissue optics is needed to determine absolute electron transport rates in corals. A potential future approach could see a combination of microfiber-PAM measurements over different wavelengths, and/or multilayered fluorescence models (see e.g. Evans, 2009) to account for different light penetration and thus different operational tissue volumes contributing to PAM measurements at different wavelengths. Expanding the applicability of PAM-based fluorescence parameters to investigate absolute electron transport is an important step towards an improved means to better characterise and hence understand how coral productivity varies over space and time.

Contributions

MS, DW, AL, US, MK and PR designed the experiments, MS, DW and BT performed the experiments, MS, DW, AL, US, DS and MK analysed and interpreted the data, MS and DW wrote the paper with the contribution of all co-authors, PR, MK contributed to reagents/materials, analysis tools.

Acknowledgements

This work was supported by the Danish Council for Independent Research / Natural Science (MK) and the Carlsberg Foundation (MK), the Australian Research Council (MS, PR) and a postgraduate scholarship from the University of Technology, Sydney (DW). Lars F. Rickelt is thanked for construction of scalar irradiance microsensors.

References

Dove, S.G., Lovell, C., Fine, M., Deckenback, J., Hoegh-Guldberg, O.V.E., Iglesias-Prieto, R., Anthony, K., 2008. Host pigments: potential facilitators of photosynthesis in coral symbioses. *Plant Cell Environ.* 31, 1523-1533.

Enriquez, S., Mendez, E.R., Iglesias-Prieto, R., 2005. Multiple scattering on coral skeletons enhances light absorption by symbiotic algae. *Limnol. Oceanogr.* 50, 1025-1032.

Evans, J. R., 2009. Potential errors in electron transport rates calculated from chlorophyll fluorescence as revealed by a multilayer leaf model. *Plant Cell Physiol.* 50, 698-706.

545 Gorbunov, M.Y., Kolber, Z.S., Lesser, M.P., Falkowski, P.G., 2001. Photosynthesis and
546 photoprotection in symbiotic corals. *Limnol. Oceanogr.* 46, 75-85.
547 Guillard, R.R.L., 1975. Culture of phytoplankton for feeding marine invertebrates, in: Smith, W.L. and
548 Chanley, M.H. (Eds.), Culture of Marine Invertebrate Animals. Plenum Press, New York, pp.
549 26-60.
550 Hennige, S.J., Suggett, D.J., Warner, M.E., McDougall, K.E., Smith, D.J., 2009. Photobiology of
551 Symbiodinium revisited: bio-physical and bio-optical signatures. *Coral Reefs* 28, 179-195.
552 Hennige, S.J., McGinley, M.P., Grottoli, A.G., Warner, M.E., 2011. Photoinhibition of Symbiodinium
553 spp. within the reef corals Montastraea faveolata and Porites astreoides: implications for coral
554 bleaching. *Mar. Biol*. 158, 2515-2526.
555 Hill, R., Larkum, A.W.D., Frankart, C., Kühl, M., Ralph, P.J., 2004. Loss of functional Photosystem II
556 reaction centres in zooxanthellae of corals exposed to bleaching conditions: using
557 fluorescence rise kinetics. *Photosynth. Res.* 82, 59-72.
558 Hill, R., Ulstrup, K.E., Ralph, P.J., 2009. Temperature induced changes in thylakoid membrane
559 thermostability of cultured, freshly isolated, and expelled zooxhanthellae from scleractinian
560 corals. *B. Mar. Sci.* 85, 223-244.
561 Hoegh-Guldberg, O., Mumby, P.J., Hooten, A.J., Steneck, R.S., Greenfield, P., Gomez, E., Harvell,
562 C.D., Sale, P.F., Edwards, A.J., Caldeira, K., Knowlton, N., Eakin, C.M., Iglesias-Prieto, R.,
563 Muthiga, N., Bradbury, R.H., Dubi, A., Hatziolos, M.E., 2007. Coral reefs under rapid climate
564 change and ocean acidification. *Science* 318, 1737-1742.
565 Iglesias-Prieto, R., Govind, N., Trench, R., 1993. Isolation and characterization of three membrane-
566 bound chlorophyll-protein complexes from four dinoflagellate species. *Phil. Trans. Royal Soc.*
567 *Lon. Ser. B: Biol. Sci.* 340, 381-392.
568 Kinzie, R.A., Jokiel, P.L., York, R., 1984. Effects of light of altered spectral composition on coral
569 zooxanthellae associations and on zooxanthellae invitro. *Mar. Biol.* 78, 239-248.
570 Koblizek, M., Kaftan, D., Nedbal, L., 2001. On the relationship between the non-photochemical
571 quenching of the chlorophyll fluorescence and the Photosystem II light harvesting efficiency.
572 A repetitive flash fluorescence induction study. *Photosynth. Res.* 68, 141-152.

573 Kolber, Z.S., Prasil, O., Falkowski, P.G., 1998. Measurements of variable chlorophyll fluorescence
574 using fast repetition rate techniques: defining methodology and experimental protocols.
575 *Biochim. Biophys. Acta – Bioenerg.* 1367, 88-106.
576 Kühl, M., Jørgensen, B.B., 1994. The light field of micro-benthic communities: radiance distribution
577 and microscale optics of sandy coastal sediments. *Limnol. Oceanogr.* 39, 1368-1398.
578 Kühl, M., Cohen, Y., Dalsgaard, T., Jørgensen, B.B., Revsbech, N.P., 1995. Microenvironment and
579 photosynthesis of zooxanthellae in scleractinian corals studied with microsensors for O_2, pH
580 and light. *Mar. Ecol. Prog. Ser.* 117, 159-172.
581 Lassen, C., Ploug, H., Jørgensen, B.B., 1992. A fiberoptic scalar irradiance microsensor - application
582 for spectral light measurement in sediments. *FEMS Microbiol. Ecol*. 86, 247-254.
583 Lavergne, J., Trissl, H.W., 1995. Theory of fluorescence induction in Photosystem-II - derivation of
584 analytical expressions in a model including exciton-radical-pair equlibrium and restricted
585 energy-transfer bewteen photosynthetic units. *Biophys. J.* 68, 2474-2492.
586 Lesser, M.P., 2000. Depth-dependent photoacclimatization to solar ultraviolet radiation in the
587 Caribbean coral Montastraea faveolata. *Mar. Ecol. Prog. Ser*. 192, 137-151.
588 Levy, O., Dubinsky, Z., Achituv, Y., 2003. Photobehavior of stony corals: responses to light spectra
589 and intensity. *J. Exp. Biol.* 206, 4041-4049.
590 Ley, A.C., Mauzerall, D.C., 1982. Absolute absorption cross-sections for photosystem-II and the
591 minimum quantum requirement for photosynthesis in *Chlorella vulgaris*. *Biochim. Biophys.*
592 *Acta* 680, 95-106.
593 Marcelino, L.A., Westneat, M.W., Stoyneva, V., Henss, J., Rogers, J.D., Radosevich, A., Turzhitsky,
594 V., Siple, M., Fang, A., Swain, T.D., Fung, J., Backman, V., 2013. Modulation of light-
595 enhancement to symbiotic algae by light-scattering in corals and evolutionary trends in
596 bleaching. *PLOS One* 8, e61492.
597 Mass, T., Kline, D.I., Roopin, M., Veal, C.J., Cohen, S., Iluz, D., Levy, O., 2010. The spectral quality of
598 light is a key driver of photosynthesis and photoadaptation in *Stylophora pistillata* colonies
599 from different depths in the Red Sea. *J. Exp. Biol.* 213, 4084-4091.
600 Oxborough, K., Moore, C.M., Suggett, D.J., Lawson, T., Chan, H.G., Geider, R.J., 2012. Direct
601 estimation of functional PSII reaction center concentration and PSII electron flux on a volume

602 basis: a new approach to the analysis of Fast Repetition Rate fluorometry (FRRf) data.
603 *Limnol. Oceanogr. Meth.* 10, 142-154.
604 Petrou, K., Jimenez-Denness, I., Chartrand, K., McCormack, C., Rasheed, M., Ralph, P.J., 2013.
605 Seasonal heterogeneity in the photophysiological response to air exposure in two tropical
606 intertidal seagrass species. *Mar. Ecol. Prog. Ser.* 482, 93–106.
607 Ragni, M., Airs, R.L., Hennige, S.J., Suggett, D.J., Warner, M.E., Geider, R.J., 2010. PSII
608 photoinhibition and photorepair in Symbiodinium (Pyrrhophyta) differs between thermally
609 tolerant and sensitive phylotypes. *Mar. Ecol. Prog. Ser.* 406, 57-70.
610 Ralph, P.J., Gademann, R., Larkum, A.W.D., Schreiber, U., 1999. *In situ* underwater measurements
611 of photosynthetic activity of coral zooxanthellae and other reef-dwelling dinoflagellate
612 endosymbionts. *Mar. Ecol. Prog. Ser.* 180, 139-147.
613 Schreiber, U., 2004. Pulse-Amplitude (PAM) fluorometry and saturation pulse method, in:
614 Papageorgiou, G., Govindjee (Eds.), *Chlorophyll fluorescence: A signature of Photosynthesis*.
615 Kluwer Academic Publishers, Dordrecht, The Netherlands, pp. 279-319.
616 Schreiber, U., Klughammer, C., 2013. Wavelength-dependent photodamage to *Chlorella* investigated
617 with a new type of multi-color PAM chlorophyll fluorometer. Photosynth. Res. 114, 165-177.
618 Schreiber, U., Klughammer, C., Kolbowski, J., 2011. High-end chlorophyll fluorescence analysis with
619 the MULTI-COLOR-PAM. I. Various light qualities and their applications. *PAM Application*
620 *Notes* 1, 1-19.
621 Schreiber, U., Klughammer, C., Kolbowski, J., 2012. Assessment of wavelength-dependent
622 parameters of photosynthetic electron transport with a new type of multi-color PAM
623 chlorophyll fluorometer. *Photosynth. Res.* 113, 127-144.
624 Smith, E.G., D'Angelo, C., Salih, A., Wiedenmann, J., 2013. Screening by coral green fluorescent
625 protein (GFP)-like chromoproteins supports a role in photoprotection of zooxanthellae. *Coral*
626 *Reefs* 32, 463-474.
627 Strasser, R., Govindjee, 1992. On the O-J-I-P fluorescence transient in leaves and D1 mutants of
628 *Chlamydomonas reinhardtii*. *Photosynth. Res.* 34, 135-135.

629 Suggett, D.J., MacIntyre, H.L., Geider, R.J., 2004. Evaluation of biophysical and optical
630 determinations of light absorption by photosystem II in phytoplankton. *Limnol. Oceanogr.*
631 *Meth*. 2, 316-332.
632 Suggett, D.J., Moore, C.M., Hickman, A.E., Geider, R.J., 2009. Interpretation of fast repetition rate
633 (FRR) fluorescence: signatures of phytoplankton community structure versus physiological
634 state. *Mar. Ecol. Prog. Ser.* 376, 1-19.
635 Suggett, D.J., Moore, C.M., Geider, R.J., 2011. Estimating aquatic productivity from active
636 fluorescence measurements, in: Suggett, D.J., Prášil, O., Borowitzka, M.A. (Eds.), *Chlorophyll*
637 *a Fluorescence in Aquatic Sciences: Methods and Applications*. Springer, The Netherlands,
638 pp. 103-127.
639 Teran, E., Mendez, E.R., Enriquez, S., Iglesias-Prieto, R., 2010. Multiple light scattering and
640 absorption in reef-building corals. *Appl. Opt.* 49, 5032-5042.
641 Wangpraseurt, D., Larkum, A.W.D., Ralph, P.J., Kühl, M., 2012. Light gradients and optical
642 microniches in coral tissues. *Front. Microbiol.* 3, 316.
643 Wangpraseurt, D., Larkum, A.W.D., Franklin, J., Szabó, M., Ralph, P.J., Kühl, M., 2014. Lateral light
644 transfer ensures efficient resource distribution in symbiont-bearing corals. *J. Exp. Biol.* 217,
645 489-498.
646 Warner, M.E., Lesser, M.P., Ralph, P.J., 2011. Chlorophyll fluorescence in reef building corals, in:
647 Suggett, D.J., Prášil, O., Borowitzka, M.A. (Eds.), *Chlorophyll a Fluorescence in Aquatic*
648 *Sciences: Methods and Applications.* Springer, The Netherlands, pp. 209-222.
649

650 Table 1. Parameters to calculate $\sigma_{II}(\lambda)$ values of *P. damicornis* and *Symbiodinium* sp.[a]

Wavelength	F_0	I_1	**PAR**	p	J	τ	τ**(reox)**	σ_{II}
(nm)	(V)	(V)	(μmol photons m^{-2} s^{-1})			(ms)	(ms)	(nm^2)
651 *P. damicornis*								
440	1.192	2.267	1050	0.432	0.760	0.327	0.354	4.46
480	1.234	2.346	1227	0.432	0.760	0.338	0.354	3.60
540	1.436	2.678	2254	0.432	0.760	0.31	0.354	2.14
590	1.373	2.606	3074	0.432	0.760	0.325	0.354	1.47
625	1.547	3.043	3256	0.432	0.760	0.323	0.354	1.32
652 *Symbiodinium* sp.								
440	1.104	2.584	942	0.529	1.124	0.283	0.499	6.23
480	1.022	2.098	1110	0.529	1.124	0.312	0.499	4.80
540	1.186	2.269	2112	0.529	1.124	0.315	0.499	2.50
590	1.082	2.159	4827	0.529	1.124	0.289	0.499	1.19
625	1.078	2.224	4373	0.529	1.124	0.285	0.499	1.33

653

654 [a] Representative data from consecutive measurements of the O–I_1 rise kinetics in *Pocillopora*
655 *damicornis* and *Symbiodinium sp.* F_0, minimal fluorescence obtained by measuring light when Q_A was
656 completely oxidised; I_1, fluorescence obtained upon actinic light+single turnover flash, when Q_A was
657 completely reduced; PAR, applied PAR to attain constant τ values; τ, time constant of Q_A^- reduction;
658 τ(reox), time constant of Q_A reoxidation. τ curves were fitted separately for the five wavelengths,
659 whereas parameters of τ(reox) (time constant of Q_A oxidation) and J (connectivity) were fixed since
660 they are independent of the wavelength (see Materials and Methods).

***Contribution**

Author contributions

MS, DW, AL, US, MK and PR designed the experiments, MS, DW and BT performed the experiments, MS, DW, AL, US, DS and MK analysed and interpreted the data, MS and DW wrote the paper with the contribution of all co-authors, PR, MK contributed to reagents/materials, analysis tools.

Fig 1

Click here to download high resolution image

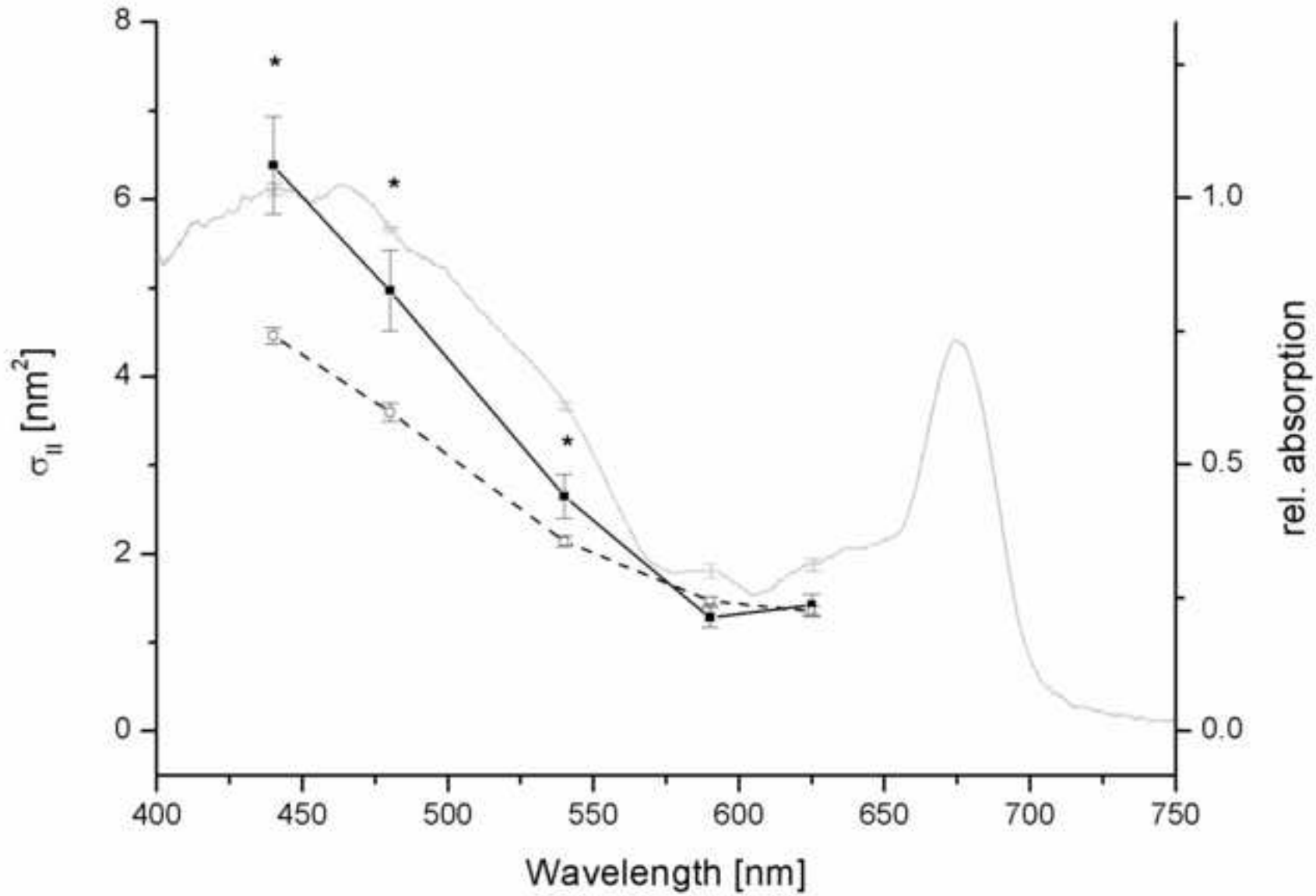

Fig 2

Click here to download high resolution image

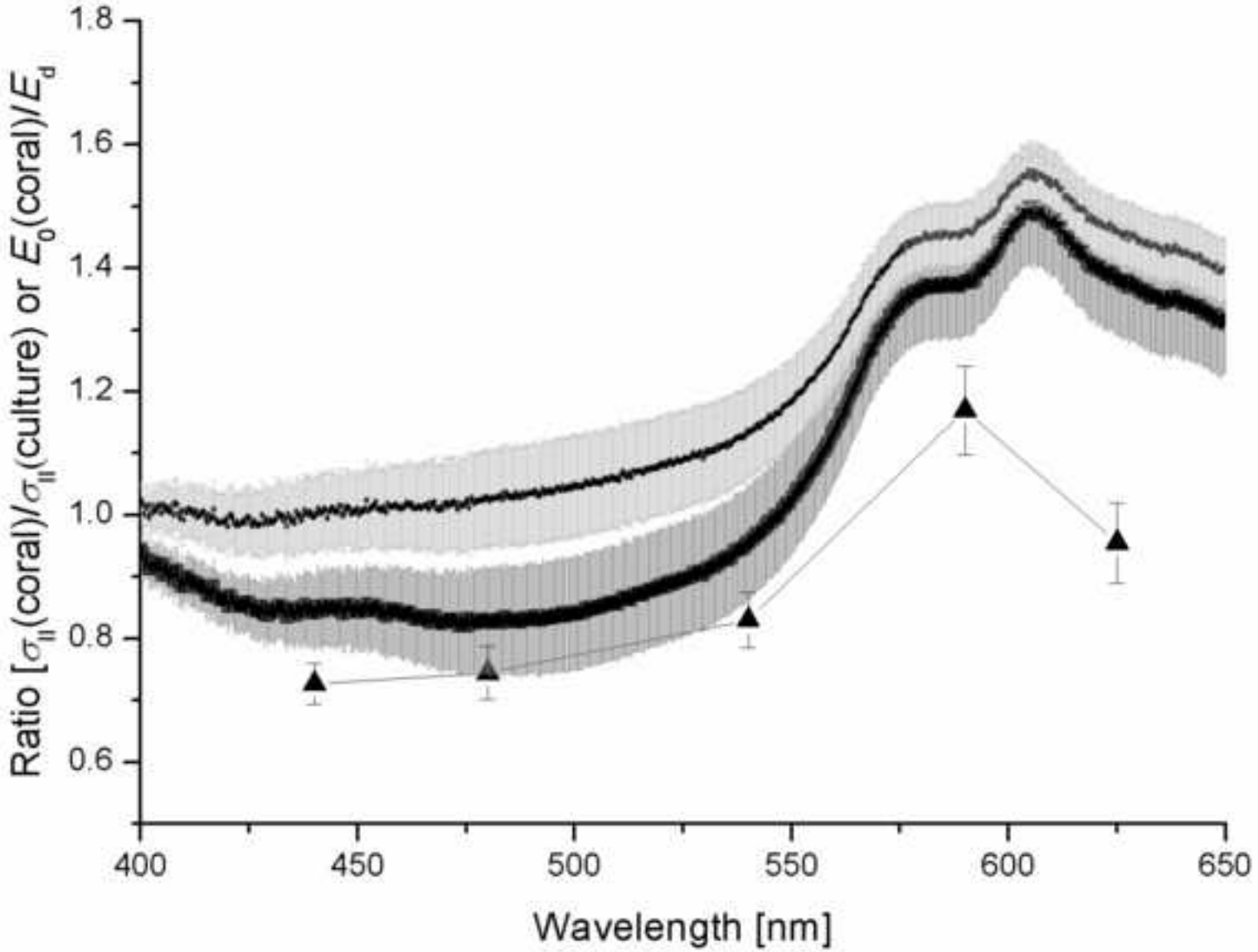

Fig 3

Click here to download high resolution image

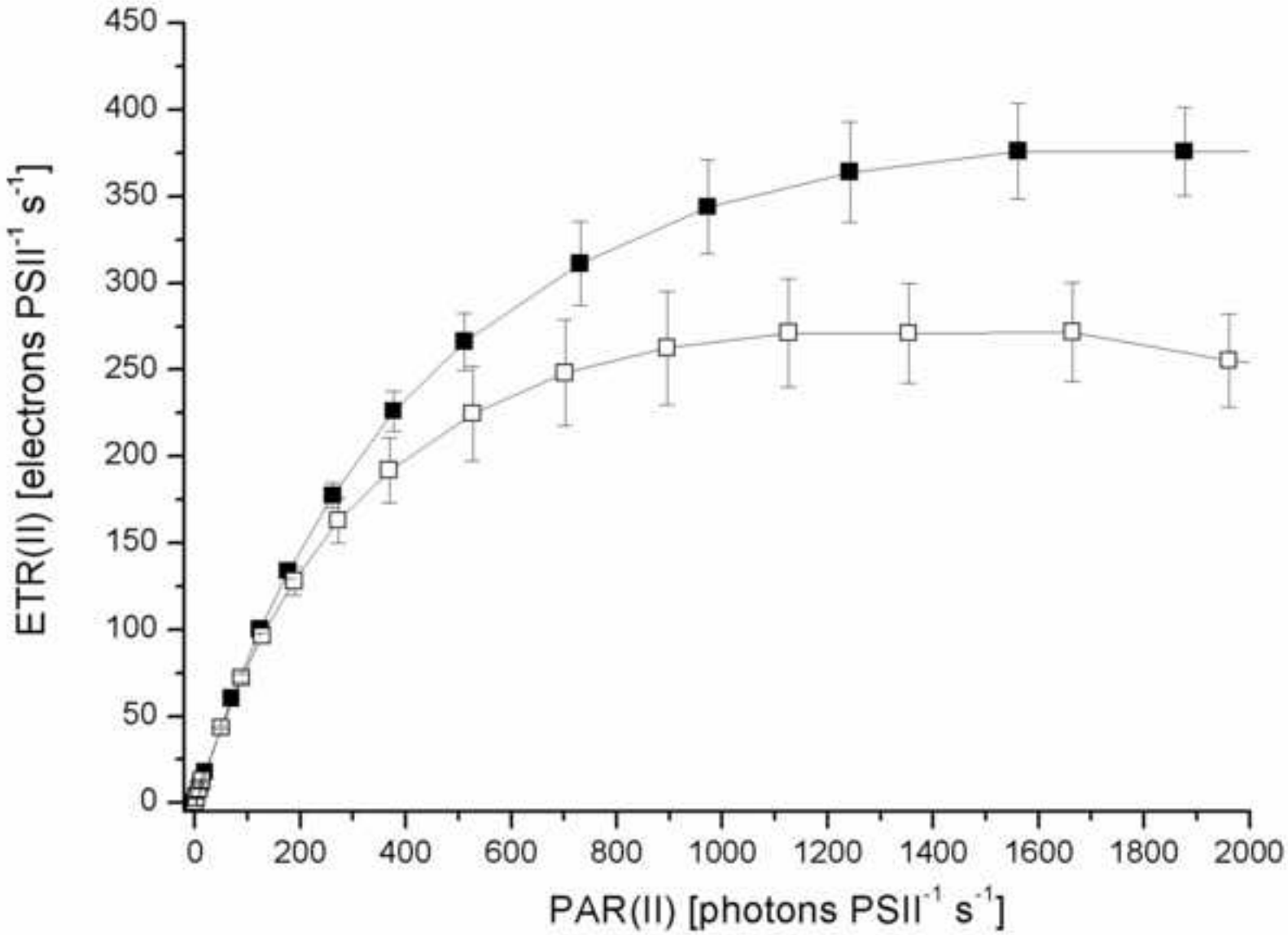

Fig 4

Click here to download high resolution image

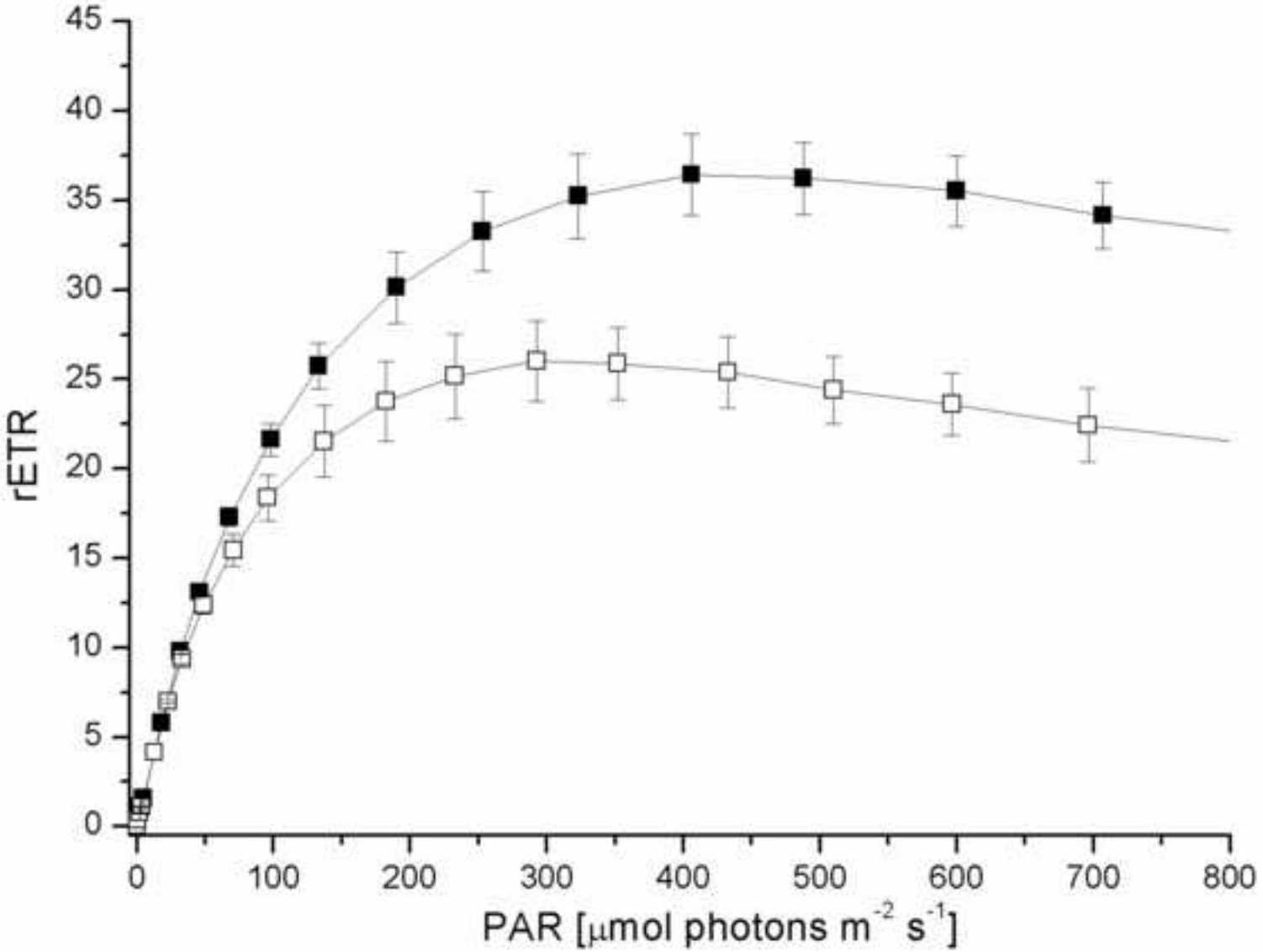

Figure legends

Fig. 1 Wavelength-dependent absorption cross section of PSII, $\sigma_{II}(\lambda)$ in cultured *Symbiodinium* sp. cells (closed squares, solid line) and in coral *Pocillopora damicornis* (open squares, dashed line). $\sigma_{II}(\lambda)$ was derived from automated measurements of five consecutive O–I_1 rise curves for each colour in the presence of far-red background light. Each transient was averaged 5-10 times in order to improve the signal-to-noise ratio. The interval between consecutive O–I_1 measurements was 10 s. $\sigma_{II}(\lambda)$ values were derived by the PamWin-3 O-I_1 fitting routine (Walz GmbH, Effeltrich, Germany). Symbols and error bars represent the average ± S.E. (n=15). * denotes statistically significant differences of $\sigma_{II}(\lambda)$ based on paired sample t-test (Pχ0.05). Relative absorption spectrum of *Symbiodinium sp.* (normalised to 1 at its maximum at ~475 nm, grey line). The spectrum is an average of 4 replicate measurements and S.E. is shown at 440, 480, 540, 590 and 625 nm.

Fig. 2 Effect of coral optics on the ratios of $\sigma_{II}(\lambda)$ of *Symbiodinium*. The figure shows the ratio of $\sigma_{II(coral)}/\sigma_{II(suspension)}$ (triangles) vs. the ratio of scalar irradiance/incident downwelling irradiance at 80 µm tissue depth (thick line) and at mean tissue depth (thin line). Standard errors (S.E.) of the scalar irradiance spectra at 80 µm and at mean tissue depths and the $\sigma_{II}(\lambda)$ ratios are shown in dark and light grey and black vertical lines, respectively

Fig. 3 Steady-state light curves of ETR_{II} recorded at 440 nm of *Pocillopora damicornis* as a function of PAR_{II} that was obtained based either on E_d (closed squares) or on E_0(calc) (open squares)

Fig. 4 Steady-state rel. ETR light curves recorded at 440 nm of *Pocillopora damicornis* as a function of either E_d (closed squares) or E_0(calc) (open squares)